

Experimental Study on the Diffusion Law of Coal-Based Solid Waste Slurry with Grouting Filling in the Gangue Voids of the Caving Zone

He Xiang, Wei Zhen,* Yang Ke, Yu Xiang, He Shuxin, Shen Yihao, and Liu Bin



Cite This: *ACS Omega* 2024, 9, 264–275



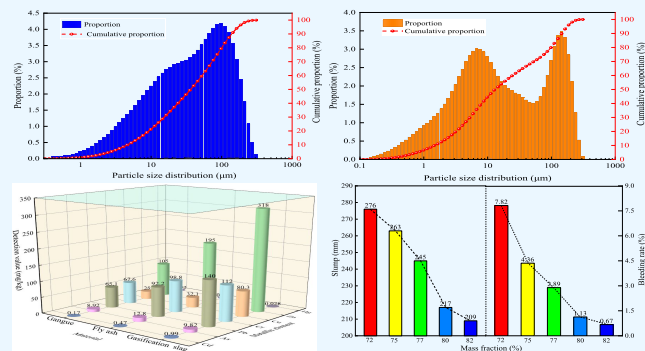
Read Online

ACCESS |

Metrics & More

Article Recommendations

ABSTRACT: Due to the concealment of the caving zone, it is difficult to detect and grasp the diffusion law of the slurry in the voids of the gangue pile. On the preparation of reasonable grouting filling materials, a large-scale three-dimensional gangue grouting filling test system has been established to detect the slurry pressure and resistivity inside the gangue pile and analyze the flow pattern of the slurry in the voids of the gangue pile. The research results show that the slump and bleeding rate of the filling slurry are significantly reduced with the increase of the fly ash content. The optimal ratio of fly ash, coal gangue, and gasification slag is 7:2:1, with a mass fraction of 72%. In the process of grouting, the internal pressure of the gangue pile can be divided into the initial stable stage, the step growth stage, and the pressure stability stage, and the change curve of the pressure sensor at the lower level is similar. The resistance value of the original broken gangue in the experiment is approximately 1600 Ω . Grouting filling forms a slurry–rock mixture, and its resistance continuously decreases with the stable injection of the slurry (minimum value 150 Ω). It is determined that the slurry near the grouting hole mainly diffuses longitudinally with a good void filling effect. The void channels of slurry diffusion are randomly distributed and have different shapes, which hinder slurry flow and diffusion. Slurry particles accumulate and settle at local small voids. Meanwhile, the surface of the gangue blocks is dry, and the slurry absorbs part of the water during diffusion, resulting in the increase of the slurry concentration and the weakening of the lateral diffusion ability. Secondary or multiple grouting can effectively fill the void of the broken gangue and further improve the filling effect.



1. INTRODUCTION

Coal is China's main energy source and important raw material, providing more than 70% of primary energy for the country's economic and social development and making indelible historical contributions to the great rejuvenation of the Chinese nation. At the same time, the coal industry has been keeping up with the pace of the times, adhering to reform, and opening up. The high-intensity development and utilization of coal resources have caused surface subsidence, roof hazards, and solid waste accumulation, which have seriously influenced the high-quality coordinated development of the ecological environment and resource recovery in the coal mining area.^{1–3} Filling mining has become a significant development direction for safe, green, and low-carbon coal mining, with abundant advantages in coal safety mining, ecological environment protection, engineering disaster prevention and control, and solid waste disposal and utilization.⁴

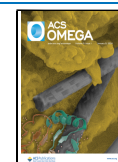
In the aspect of the caving zone grouting practice, the relationship and control mechanism between grouting and filling in the caving zone and rock movement were studied.^{5–7} To address the ecological environment degradation caused by

the discharge of gangue in the Hancheng mining area, Li et al.⁸ explored the residual spatial distribution characteristics of goaf in the experimental working face and proposed a high- and low-level collaborative fluidized filling mining method. Li et al.⁹ compared and analyzed the movement characteristics of the overlying strata in strip mining and caving zone grouting filling mining through physical simulation experiments. The coal pillar grouting filling structure can effectively control surface subsidence. Zhang et al.¹⁰ expounded the current situation of waste disposal and utilization in China and put forward the subsequent space gangue grouting filling method in coal mines in view of the space–time interference between solid waste filling and coal mining. Zhao et al.¹¹ put forward the real-time detection method of the grouting filling effect and quantified

Received: June 27, 2023

Accepted: October 4, 2023

Published: December 15, 2023



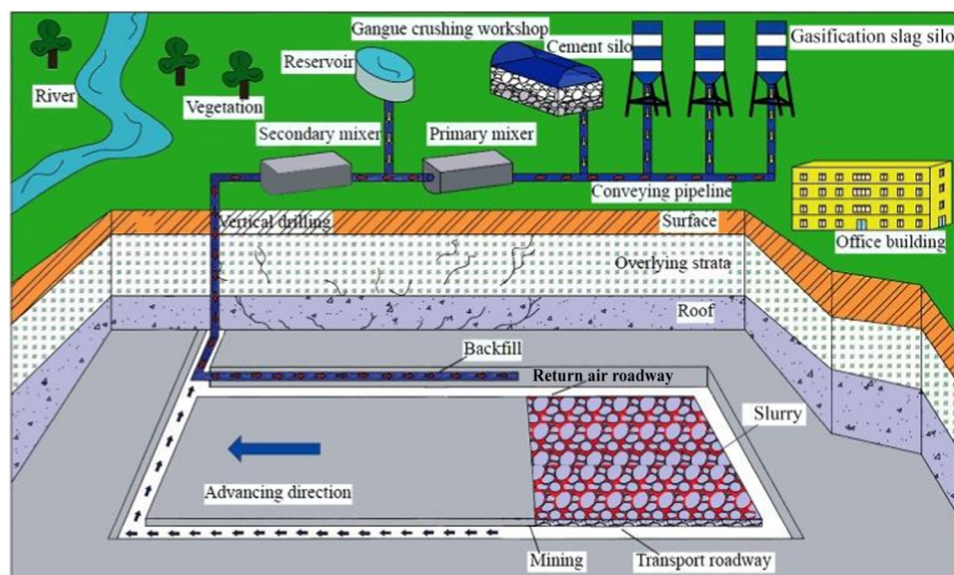


Figure 1. Schematic diagram of coal-based solid waste grouting filling mining.

the evaluation index in combination with the grouting filling project in strip mining of coal mines.

At present, there is no independent and comprehensive theoretical system for the grouting filling theory, and it is usually based on the grouting theory of fractured rock or soil. Infiltration grouting is to simplify the slurry into Newtonian fluid. The development of Newton's fluid uniform motion diffusion theory, Newton's fluid deceleration motion diffusion theory, and time-varying fluid diffusion theory, all obey the linear Darcy's infiltration law.^{12,13} Split grouting is the high-pressure injection of cement or chemical slurry into the formation, improving its properties, integrity, and strength.^{14,15} Fractured rock mass grouting refers to the high-pressure injection of grout into complex and variable rock and soil fractures to prevent the instability and failure of underground engineering fractured rock masses. Compaction grouting refers to the injection of cement or chemical slurry into the soft soil layer to control surface subsidence, and the best compaction area is located in the weakest soil layer.^{16,17}

The simulation experiment is the most commonly used method to study the effect of grouting filling. Yang et al.¹⁸ developed static pressure grouting and vibration grouting simulation devices and analyzed the slurry diffusion law and grouting mechanism under static and dynamic water pressures. Feng et al.¹⁹ independently designed a three-dimensional constant pressure osmotic grouting test device, studied the relationship between confining the pressure, permeability coefficient, and slurry viscosity, and discussed the grouting sealing mechanism of the broken rock mass. Miwen et al.²⁰ developed a high-pressure grouting test system and analyzed the diffusion characteristics of the grouting slurry under a high-pressure closed environment. Zhang et al.²¹ developed a single crack, double crack, and three-dimensional orthogonal crack network grouting test system and analyzed the grouting diffusion characteristics of the chemical and cement slurry at different temperatures. Based on the rock mass structure in the water-rich fracture zone, Li et al.²² proposed dominant split grouting and established the grouting diffusion control equation, considering the rheological properties of the grout. Wang et al.²³ carried out slurry diffusion simulation tests

through the self-developed fissure grouting test platform, obtained the characteristics of the slurry concentration distribution along the diffusion path, and discussed the formation mechanism of the slurry concentration differential distribution based on Newton's fluid theory. Sha et al.²⁴ compared and analyzed the changes in the diffusion morphology and retention rate of the cement-water glass slurry and polymer-modified cement slurry and proposed the mechanism of partition and layered diffusion of the cement slurry. Zhang et al.²⁵ studied the relationship between the flow velocity and the slurry diffusion distance through laboratory tests and obtained that the flow velocity was inversely proportional to the grouting consolidation area. Ao et al.²⁶ simulated the grouting filling in the goaf of coal mines to reduce the development of water-conducting cracks in the overlying strata and analyzed the effectiveness and stability of grouting filling in goafs. Zou²⁷ obtained from the test that the slurry diffusion form of grouting filling in the caving zone is "spine type", and the slurry diffusion distribution in the accumulation zone is "floc type". Zhu et al.²⁸ built a model of broken gangue in the caving zone and studied the diffusion law of the gangue slurry in the broken rock space. Qiu et al.²⁹ studied the flow and sedimentation of the filling slurry and the distribution of slurry particle mass fraction and proposed a strength evaluation method for grouting filling bodies in collapsed zones. As shown in Figure 1, grouting filling in the caving zone means injecting filling materials into the voids of broken gangue in goaf under high pressure to fill and strengthen rock blocks and control rock movement and surface subsidence, which can better solve the problems of project safety and environmental pollution caused by solid waste discharge. Grouting filling in the caving zone is a hidden project with complexity and unpredictability, and the mechanisms of slurry diffusion and slurry–rock interaction cannot be obtained directly. The relevant theoretical research lags behind engineering practices.

Favorable research results were achieved with laboratory tests and theoretical analysis. However, simplified theoretical and experimental models are difficult to accurately reflect on-site grouting filling, and the theory of slurry diffusion in the

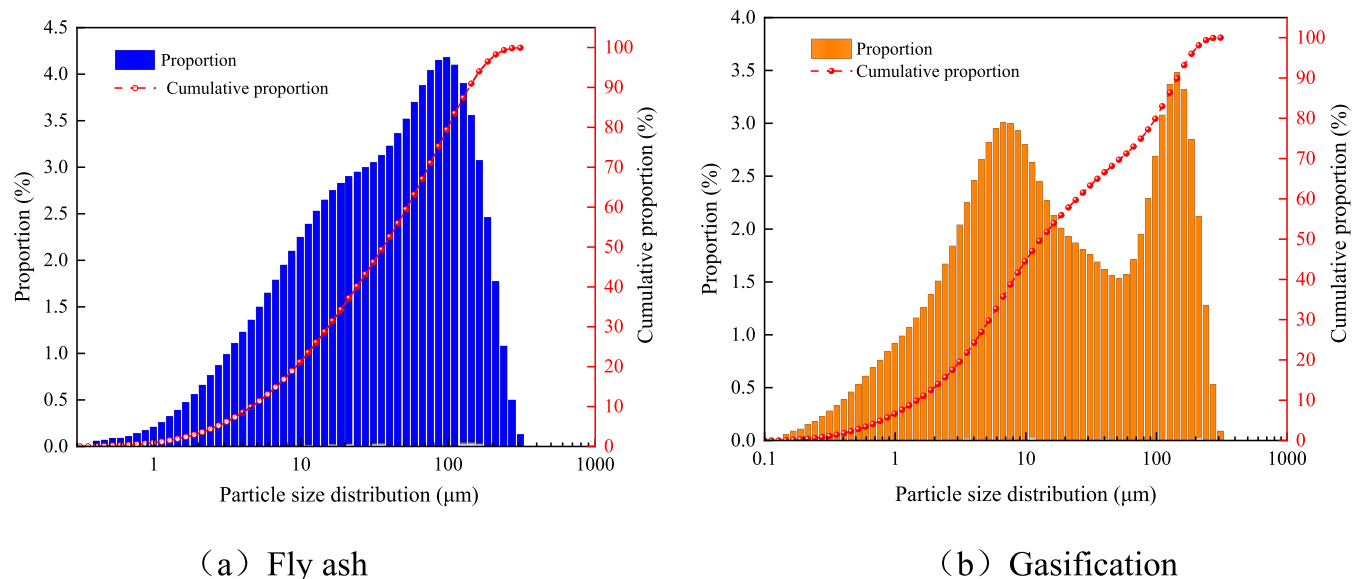


Figure 2. Particle size distribution of the filling material.

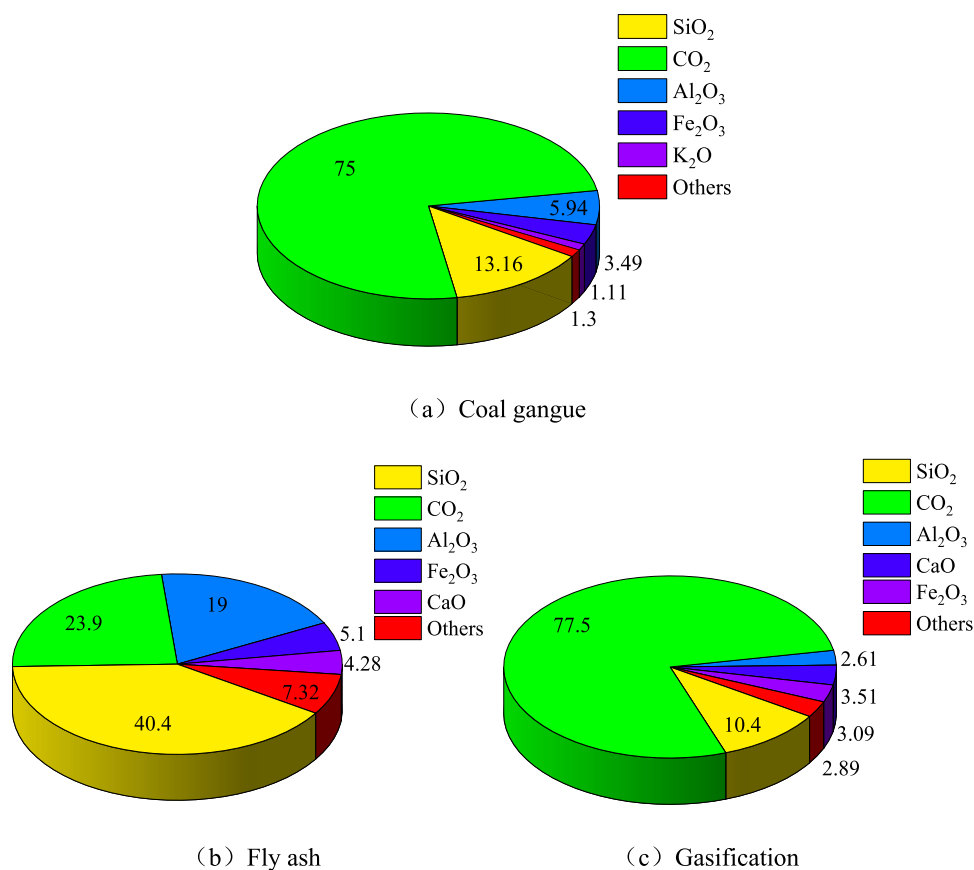


Figure 3. Oxide content of the filling material.

voids of the gangue blocks is still incomplete because of the complexity and invisibility of the void structure of the gangue in goaf. A large-scale simulation experiment was carried out on the internal grouting filling of gangue voids, and the diffusion law of the grouting filling slurry for broken gangue under different factors was analyzed in detail, which further supplements and improves the current theory and technology of grouting filling for broken gangue in goaf.

2. PHYSICAL PROPERTIES OF THE FILLING SLURRY

The raw materials used to prepare the filling slurry are coal gangue, fly ash, and gasification slag. The particle size distribution and oxide content are shown in Figures 2 and 3. Coal gangue is associated with coal formation, and the occurrence environment is ever-changing. The mineral composition is complex and changeable, the main oxides are SiO_2 , Al_2O_3 , Fe_2O_3 , and K_2O . The particle size of the coal

gangue used in the test is less than 2 mm. Fly ash is a fine solid particle produced by high-temperature calcination of pulverized coal and is the main solid waste discharged from thermal power plants. The content of fly ash with particle size less than 50 and 180 μm accounts for more than 50 and 90%, respectively; the nonuniformity coefficient is 11.31, the curvature coefficient is 1.13, and the particle size distribution is uniform. The main oxides are SiO_2 , Al_2O_3 , Fe_2O_3 , and CaO , with a grayish white appearance, a density of about 2150 kg/m^3 , a fineness of about 20, and a specific surface area of about $300 \text{ m}^2/\text{kg}$. Gasification slag is the solid waste slag produced during the thermal chemical processing of coal. The proportion of gasification fine slag with particle size less than 13 and 310 μm is more than 50 and 90%, respectively; the nonuniformity coefficient is 16.62, the curvature coefficient is 0.77, the particle size distribution is uneven, and the fine grade content is too much. The main oxides are SiO_2 , Al_2O_3 , CaO , and Fe_2O_3 , and the appearance is black sand granular, which is easy to grind.

The heavy metal content of the test material is shown in Figure 4. It can be seen that compared to the "Soil

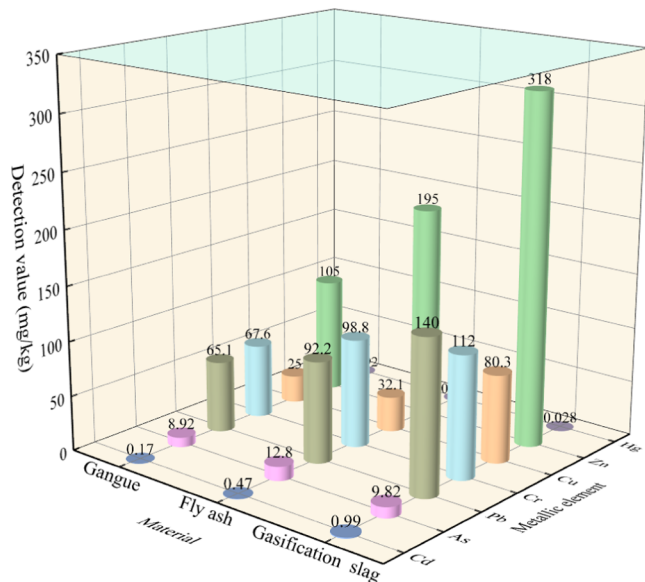


Figure 4. Heavy metal content of filling materials.

Environmental Quality Standard for Soil Pollution Risk Control of Agricultural Land (Trial)" (GB15618-2018),³⁰ the heavy metal content in gasification slag is lower than the soil pollution risk control value, meeting the requirements of the underground filling test.

Slump reflects the workability of the filling slurry and is an important indicator for measuring the fluidity of the slurry.^{31,32} Bleeding is the phenomenon of coarse aggregate sinking and water floating in the process of slurry transportation, vibration, and pumping, which is an important index to measure the effect of grouting filling. The tests were conducted on the slump and bleeding rate of the slurry under different mass fractions and filling material contents, and the test results are shown in Figure 5.

As shown in Figure 5, the slump and bleeding rate of the filling slurry continuously decrease with an increase of the coal gangue content. When the coal gangue content is 0.1 kg, the slump of the slurry is 241 mm. With the increase of the fly ash

content, the slump and bleeding rate of the slurry decreased continuously, and the bleeding rate of the slurry ranged from 1.26 to 3.88%, with a low bleeding rate. The main reason was that the increase of the fly ash content intensified the volcanic ash reaction and increased the consistency and water retention capacity of the slurry, resulting in the decrease of the slump and bleeding rate. The slump and bleeding rate of the filling slurry are inversely proportional to the gasification slag content. When the gasification slag content is 0.2 kg, the slump of the slurry is 265 mm, and the bleeding rate is 2.67%. This is mainly due to the poor hydrophilicity of gasification slag, which increases the consistency of the slurry, leading to an increase in the slump and bleeding rate. As the mass fraction of the filling slurry increased, its slump and bleeding rate decreased continuously. When the mass fraction increased from 72 to 82%, the slump of the slurry decreased by 24.27%, and the bleeding rate decreased by 91.43%, with a large range of changes due to the increase of the mass fraction of the slurry, the decrease of workability of the slurry, and the decrease of the slump and bleeding rate.

According to the results of the slurry flow test, the slurry with a mass ratio of 2:7:1 and mass fraction of 72% of coal gangue, fly ash, and gasification slag is selected as the solid waste grouting filling material. This material has better fluidity and workability.

3. EXPERIMENT DESIGN

3.1. Experimental Device and Measurement. The large-scale three-dimensional crushed gangue grouting filling test device mainly consists of a test box, a grouting system, a data acquisition system, and other parts. The actual test device is shown in Figure 6.

The gangue grouting filling test box is composed of a 3D filling box, a slurry discharge hole, a grouting hole, a base, and various valves. Among them, the three-dimensional filling box is made of a 10 mm thick acrylic material, with a length of 1200 mm, a width of 800 mm, and a height of 700 mm. Four drainage holes with an inner diameter of 40 mm are opened in front and behind at a height of 10 mm above the bottom of the box, and two grouting holes with an inner diameter of 32 mm are opened at heights of 350 and 500 mm above the bottom on the side of the box. The base of the filling box is welded from angle steel and equipped with universal wheels for easy movement. The vertical angle steel in the middle is welded to the base to fix the filling box. The grouting system is composed of a portable high-pressure grouting pump and grouting pipe. The maximum pressure of the grouting pump is 21 MPa, the maximum rated power is 1.3 kW, and the speed of the grouting pump is adjustable, up to 1440 r/min. The grouting pipe is composed of a high-pressure hose and pneumatic joint, and the pneumatic tee connects the pressure gauge and the flow meter. The data acquisition system is composed of a computer, electrode sensor, pressure sensor, data acquisition instrument, etc. The pressure and resistance values of the measuring points in this grouting filling test are collected. The pressure range is 0–0.1 MPa, the pressure acquisition period is 1s, and the collection period of the electrical instrument is 2 min. The output signal of the acquisition instrument is the quality and resistance signal. Various valves of the test device are used to control the slurry flow path of the pipeline.

The overall integrity of broken gangue in goaf is poor, the voidage is large, and the gangue blocks have their own joint development, with a wide range of particle size distribu-

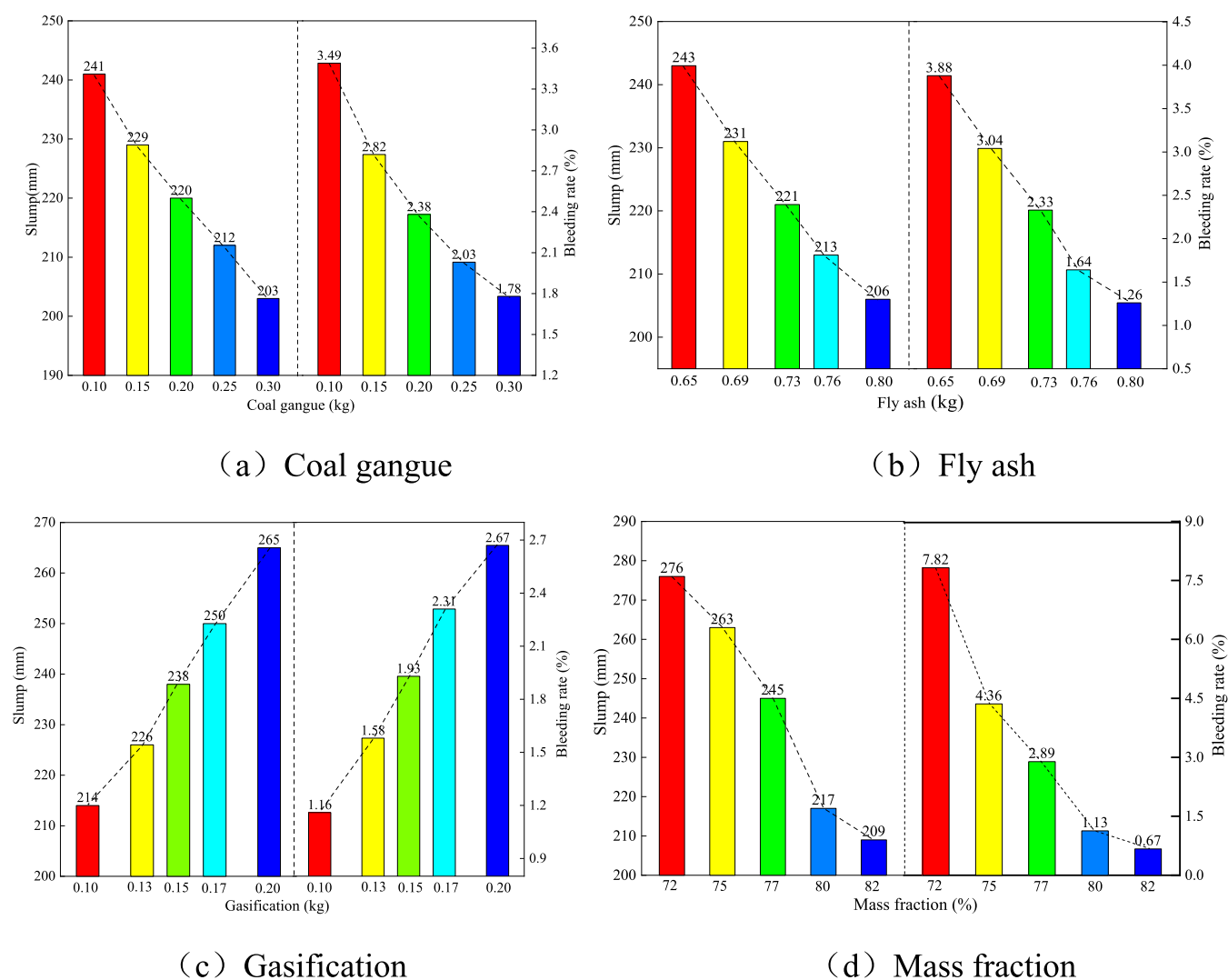


Figure 5. Slump and bleeding rate of the filling slurry.

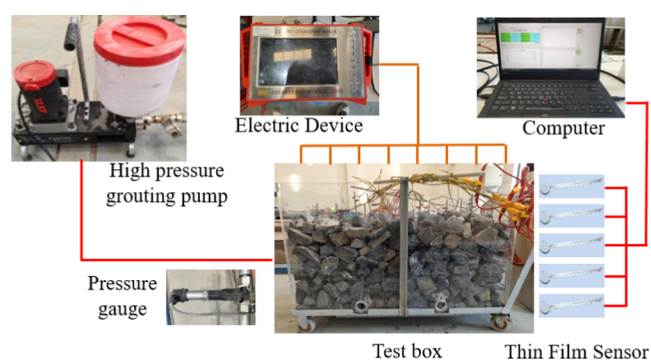


Figure 6. Physical diagram of debris grouting and the filling test device.

tion.^{33,34} According to the distribution characteristics of broken gangue in goaf investigated by the actual project, gangue with different particle sizes is used to simulate the broken rock mass in the goaf behind the support, and the broken gangue is required to be horizontally loaded into the test box. After the test box is filled with broken gangue, a voidage test is conducted. Water is injected into the test box through the grouting hole, and the water injection time and

amount are recorded when the broken gangue is flooded. Soaked for 24 h, the crushed gangue is fully saturated, the test error is reduced, and the amount of water released by weighing is measured. The water injection and discharge tests were repeated for 3 times, and the average value was taken as the overall voidage.

Based on the study of the diffusion law of the broken gangue slurry and the similarity theory, the grouting pressure is designed to be 0.6 MPa. The experimental grouting filling object is crushed gangue blocks, and the grouting material is a coal-based solid waste slurry. Before the experiment, the broken gangue blocks are filled into the test box with a loading height of 500 mm. At the same time, sensors are arranged, as shown in Figure 7, which are mainly divided into the pressure sensor arrangement and electrode arrangement.

3.2. Experimental Steps. The test steps of large-scale three-dimensional broken gangue grouting and filling mainly include test preparation, goaf simulation, voidage test, grouting and filling implementation, and filling effect evaluation. The detailed test procedure is shown in Figure 8.

3.2.1. Test Preparation. Before the experiment, 1000 kg of crushed gangue with different particle sizes, 20 thin film pressure sensors, and 16 high-density electrical instrument electrodes is prepared, and it is ensured that the sensor leads

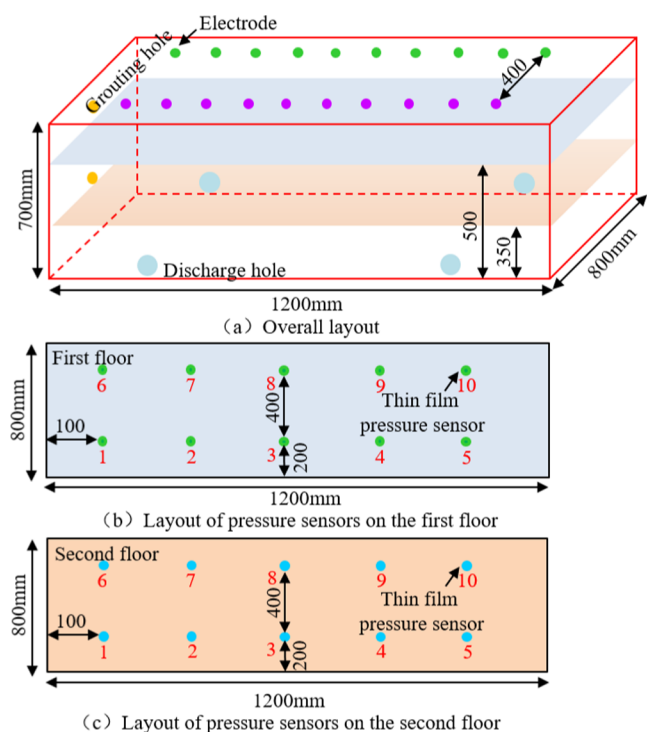


Figure 7. Layout of pressure transducers (unit: mm).

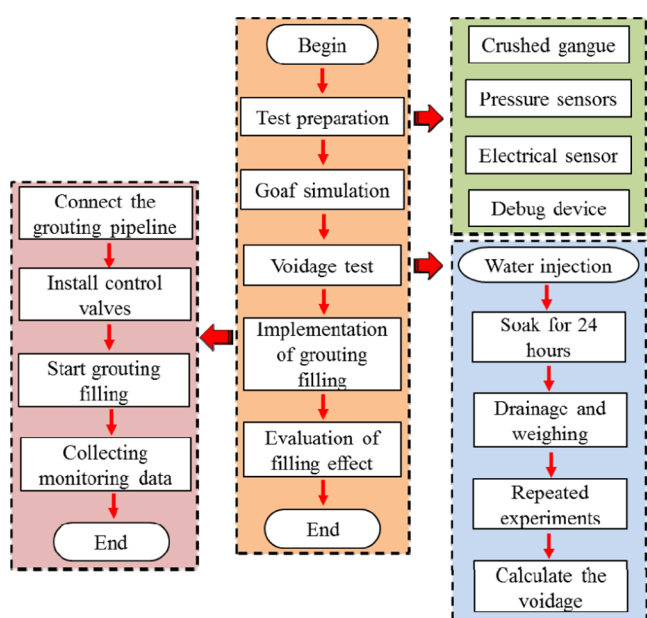


Figure 8. Test flow of grouting and filling of large-sized three-dimensional crushed gangues.

are connected properly. The grouting pipeline and high-pressure grouting pump are debugged.

3.2.2. Goaf Simulation. The broken gangue with different particle sizes is fully mixed, and then the test chamber is filled in layers to simulate the broken gangue pile in the goaf of a coal mine, as shown in Figure 6.

3.2.3. Voidage Test. After the crushed gangue is filled, the water pipe is connected to the grouting hole, and the inlet valve is opened for water injection. When there is water overflow in the drainage hole, the drainage valve is closed and the water injection is stopped. After standing for 24 h, the

drainage valve is opened, the amount of water released is measured, and the voidage is evaluated.

3.2.4. Implementation of the Grouting Filling. Before the experiment, the grouting pipe is connected with the high-pressure grouting pump and the grouting hole of the test box, the control valve is installed, and the filling slurry is prepared according to the ratio. During grouting filling, the sensor acquisition system should be started; the drainage valve at the bottom of the test chamber should be closed; the grouting pump should be opened to start grouting; and the height of the filling grout should be observed in real-time through the visual test chamber. When the slurry overflows at the top of the test chamber, the grouting pump should be closed to stop grouting filling and the grouting pipeline should be rinsed at last.

3.2.5. Evaluation of the Filling Effect. After grouting filling is completed, the electrical method is collected every 1 h until the slurry reaches its initial setting. When the slurry fully diffuses during the experiment, the effect of the grouting filling rate.

4. EXPERIMENTAL RESULT ANALYSIS

4.1. Evolution Law of Slurry Pressure at Measuring Points. In the process of grouting filling, the grouting pressure is 0.6 MPa, and the characteristics of slurry diffusion and leakage during grouting filling are observed. At the end of the test, the collected quality signal was converted into pressure, and the slurry pressure change curve of the measuring points 1# and 6# during grouting filling was obtained, as shown in Figure 9.

It can be seen from Figure 9 that the pressure of the measuring points 1# and 6# in grouting filling is increasing continuously. In the initial stage of filling, there is a sudden increase in the pressure of the slurry near the grouting outlet (measuring points 1# and 6#), and then the pressure presents a plateau stability; the pressure increases in the middle stage like a step, and the pressure is relatively stable in the later stage until the end of grouting.

According to the pressure change, the grouting filling process can be divided into three stages: the initial stable stage, the step growth stage, and the pressure stability stage. Initial stable stage: Under the driving force of grouting pressure, the value of the pressure sensor suddenly increases and then maintains a relatively stable platform trend. Then, the pressure shows a single peak change of first increasing and then decreasing. Step growth stage: The pressure as a whole presents a step-like change of stable, rising, stable, and rising. The slurry is pressed into the void channel to break the original diffusion balance, and the slurry gradually diffuses through different void paths to the pressure sensor; the pressure value shows a step rise with different rise times from the rising stages. Pressure stability stage: The diffusion movement of the slurry reaches its limit but it is not completely filled with voids in a cemented state. There are cracks at the edges, forming a diffusion movement channel for the low-concentration slurry. In the later stage of grouting, a small amount of slurry enters the edge cracks and the pressure value increases slightly. The final effect of grouting filling is determined by the step growth stage and the pressure stability stage.

In the process of the grouting filling test, the pressure sensor of the same layer with equal distance from the grouting hole has obvious followability, but the pressure increase or decrease degree is different. This is because the flow and diffusion characteristics of the slurry with the same ratio are the same;

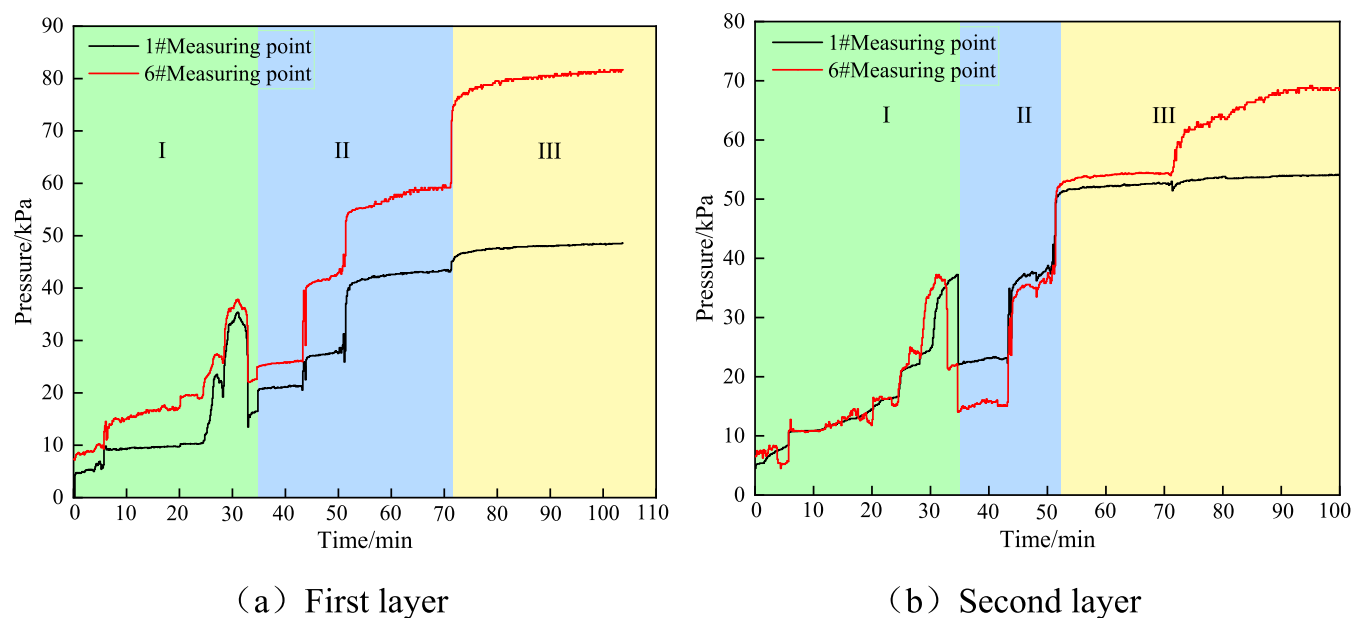


Figure 9. Slurry pressure change curve at the 1# and 6# measuring points.

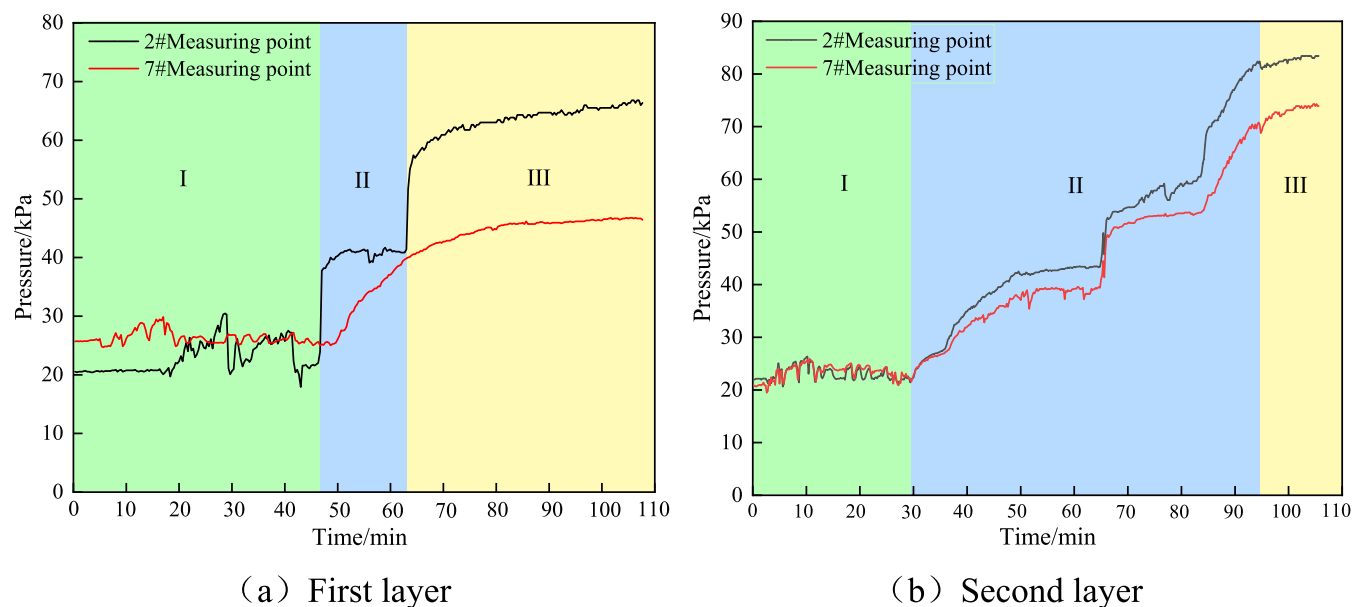


Figure 10. Slurry pressure change curve at the 2# and 7# measuring points.

that is, the time of slurry diffusion to the pressure sensor is similar under the same grouting pressure. In addition, the structure of the void formed by the accumulation of broken gangue is complicated, and the amount of slurry moving to each pressure sensor is different, which leads to the difference in the pressure value. The variation curves of pressure sensors in different layers are similar, and they all go through three stages: the initial stable stage, the step growth stage, and the pressure stability stage, but the pressure rise amplitude and duration of each stage have no obvious rules. The initial stable stage of pressure sensors at the measuring points 1# and 6# on the first layer lasts for about 35 min, the step growth stage lasts for about 37 min, and the pressure stability stage lasts for about 33 min. The initial stable stage of the pressure sensors at the measuring points 1# and 6# on the second layer lasts for about 35 min, the step growth stage lasts for about 17 min, and the

pressure stability stage lasts for about 48 min. During the test, the maximum value of the pressure sensor at the 1# and 6# measuring points of the first layer is 82.6 kPa, and the pressure stability stage is entered after 72 min of filling. The maximum value of the pressure sensor at the 1# and 6# measuring points of the second layer is 68.2 kPa, and the pressure stability stage is entered after 53 min of filling.

In the process of grouting filling, the grouting pressure is 0.6 MPa, and the characteristics of slurry diffusion and leakage during grouting filling are observed. At the end of the test, the collected quality signal is converted into pressure, and the slurry pressure change curves of the measuring points 2# and 7# during grouting filling are obtained.

As shown in Figure 10, the pressure at the measuring points 2# and 7# during grouting filling continues to increase, and there is a sudden increase of pressure near the grouting outlet

(measuring points 2# and 7#) in the initial stage of filling, and the pressure in the grouting filling process still has three stages: the initial stable stage, the step growth stage, and the pressure stability stage.

As the slurry continuously injects into the voids, the pressure at different measuring points undergoes three stages: the initial stable stage, the step growth stage, and the pressure stability stage. The initial stable stage of the pressure sensors at the measuring points 2# and 7# on the first layer lasts for about 47 min, the duration of the step growth stage lasts for about 16 min, and the duration of the pressure stability stage lasts for about 37 min. The initial stable stage of the pressure sensors at the measuring points 2# and 7# on the second layer lasts for about 30 min, the duration of the step growth stage lasts for about 65 min, and the duration of the pressure stability stage lasts for about 15 min. During the test, the maximum value of the pressure sensor at the 2# and 7# measuring points of the first layer is 66.3 kPa, and the pressure stability stage is entered after filling for 62 min. The maximum value of the pressure sensor at the 2# and 7# measuring points of the second layer is 82.6 kPa, and the pressure stability stage is entered after filling for 95 min.

4.2. Resistivity Evolution Law. Resistivity measurement is an ideal method for evaluating the filling effect, which is based on detecting the conductivity of the slurry and coal gangue, and it integrates the detection of the slurry diffusion depth and the slurry–rock boundary.^{35–38} By using a one-time arrangement of electrodes, using a CNC electrode converter and an electrical instrument, the measurement line can be quickly measured, collected, and the data can be stored. Professional software is used to draw a resistivity map that reflects the diffusion of the filling slurry, and comprehensive analysis and evaluation of the filling effect in the mine are conducted. The advantages include:

- (1) Having a comprehensive theoretical foundation and measured data, obtaining the resistivity of slurry diffusion through experiments and theory, analyzing the conductivity difference between the slurry and the surrounding rock, and using this to invert the diffusion depth of the filling slurry and the division of the slurry–rock interface.
- (2) Grouting filling mining is continuous and long-term, and slurry diffusion is a dynamic correlated process. The resistivity filling effect evaluation can monitor slurry diffusion in an all-round and real-time manner and continuously monitor the grouting filling mining process in time and space.
- (3) During electrical monitoring, the electrode arrangement is complete and convenient. Before the test, the monitoring range is determined and a one-time electrode arrangement is carried out. During the monitoring time until the end of the test, data is directly collected without changing the electrode position to obtain the variation pattern of electrical resistivity during the test process.
- (4) The collection and processing of experimental data is fast and can be quickly processed through professional software and resistivity imaging, intuitively reflecting the evolution law of electrical information during the grouting filling mining process.

Based on the working principle and advantages of the above resistivity monitoring, the concrete implementation steps of

this filling effect evaluation method are presented, as shown in Figure 11.

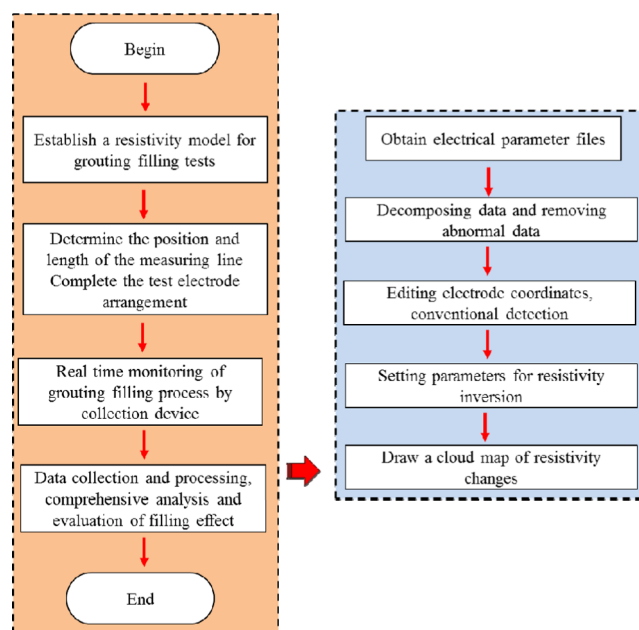


Figure 11. Evaluation steps of the resistivity filling effect.

During the test, comprehensive electrical information data were collected, and professional software was used to perform operations such as deconstructing data, removing abnormal data, editing electrode coordinates, and setting parameters. Finally, the resistivity cloud map of slurry diffusion during different periods of grouting filling was obtained, as shown in Figure 12.

As can be seen from Figure 12, the overall diffusion of the grouting filling slurry is distributed at high- and low-resistance closed or semiclosed intervals, and the resistance varies between 150 and 1600 Ω , while the low-resistance region is in dynamic change. This is due to the conductivity difference between the slurry and the rock, and the stable injection of the slurry changes the original electric field of the test box, resulting in the phenomenon of alternating high- and low-resistance areas. Analysis suggests that the low-resistance zone is a zone containing a large amount of slurry, while the high-resistance zone is a zone containing a small amount of slurry or no slurry. That is, the low-resistance zone has a good slurry diffusion motion effect, while the high-resistance zone has a poor slurry diffusion motion effect. The resistance value of the original broken gangue in the experiment is about 1600 Ω . Grouting filling forms a slurry–rock mixture, and its resistance value continuously decreases with the stable injection of the slurry, with a minimum value of 150 Ω .

Based on the collected pressure and electrical data, it can be seen that the transverse range of 0–350m and longitudinal range of $-50 \sim -350$ m of the test chamber are relatively low-resistance areas, and the low-resistance areas are constantly expanding dynamically. The slurry diffusion form is irregular and elliptical, mainly because the broken gangue used in the test is an irregular rock, resulting in differences in the size and shape of the void. The slurry has the phenomenon of flow and diffusion along the advantageous path, and the broken gangue has strong water absorption, resulting in a large amount of water being absorbed during the flow and diffusion of the

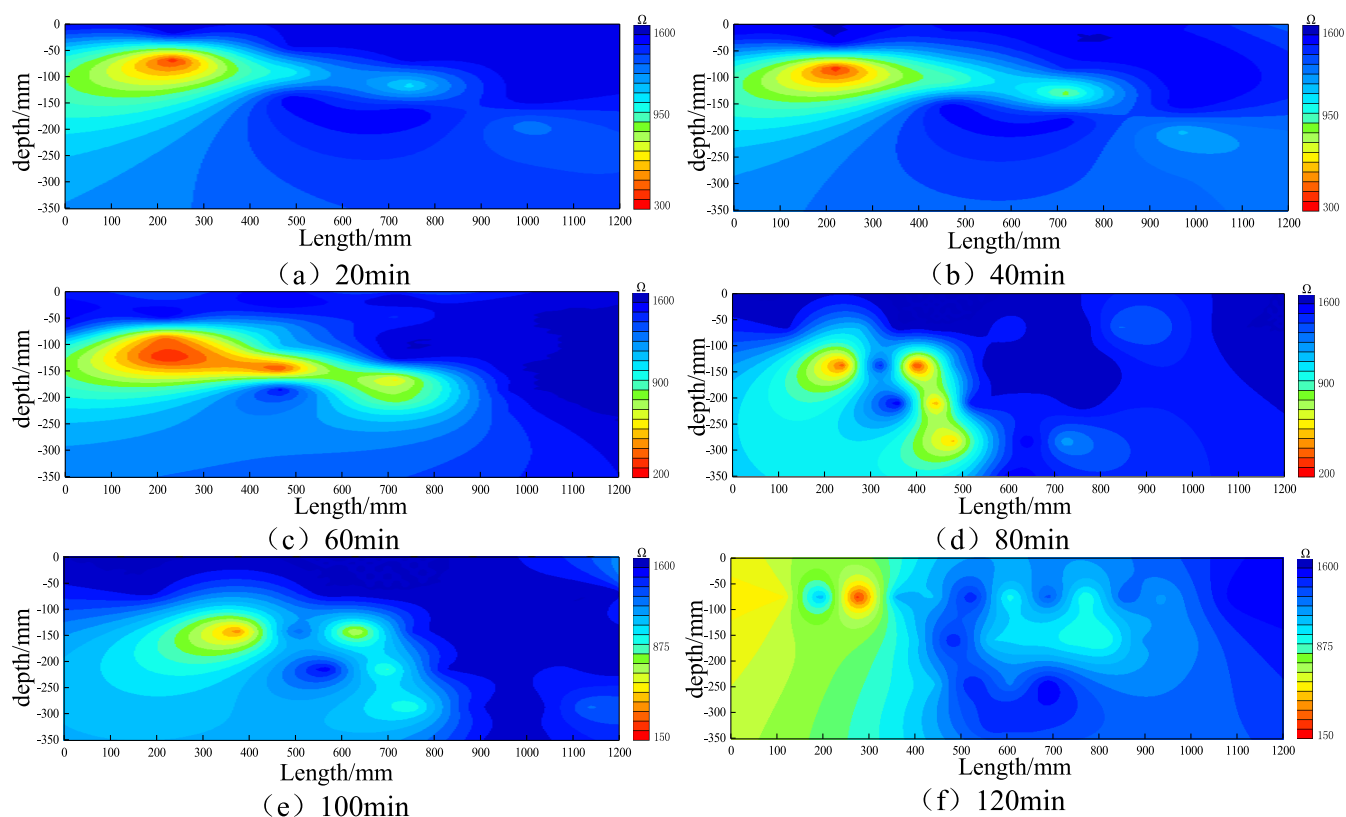


Figure 12. Cloud chart of diffusion resistivity of the grouting and filling slurry.

slurry, increasing the viscosity of the slurry and decreasing the fluidity. It is difficult to achieve an ideal diffusion. The comparison between the filling slurry and the broken gangue shows a low-resistance response. As the grouting filling stabilizes, the resistance of the slurry–rock mixture shows different numerical changes and the resistance value continuously decreases. Therefore, the filling effect can be evaluated by comparing the electrical resistance values of the slurry–rock mixtures at different time periods.

The slurry diffusion was observed during the test, and combined with the pressure and electrical monitoring, it can be seen that the slurry flows in the void of the broken gangue and the overall fluidity is good. The flow state observation of the grouting filling slurry is shown in Figure 13. The upper left corner of the figure shows the diffusion state of the slurry at the bottom of the test box.

From Figure 13, it can be seen that at the beginning of grouting, the slurry rapidly infiltrates into the bottom of the test box near the grouting hole and gradually fills the bottom gangue void. As the grouting amount gradually increases, the longitudinal diffusion form of the slurry transitions from a cylindrical shape to a conical shape centered around the grouting hole. The slurry gradually diffuses to the middle and upper part through the advantageous path, and finally the slurry emerges within the upper 350 mm range, that is, the slurry diffusion distance in the horizontal direction is 350 mm. The grouting filling test of the broken gangue is a relatively closed limited space. In the grouting simulation process, there must be water in the void of the broken gangue that does not participate in the hydration reaction, which will cause the slurry to not completely fill the void. But in the actual grouting filling project, the grouting area is an infinite extension of

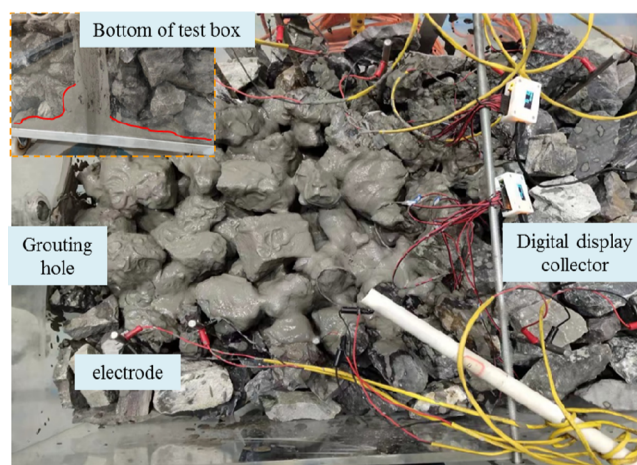


Figure 13. Grout diffusion test diagram.

three-dimensional space. Under the driving force of grouting pressure, the slurry diffuses around the void channel until the pressure is dissipated. The water in the void that does not participate in the hydration reaction gradually dissipates and loses. Secondary or multiple grouting can effectively fill the broken gangue void, further improving the filling effect of the mine.^{39–41}

4.3. Analysis of the Slurry Diffusion Law. The flow process of the grouting filling slurry before and after the test is observed and recorded, and the diffusion process of the slurry in the broken gangue body is drawn, as shown in Figure 14. It can be seen that the overall flow and diffusion of the slurry exhibit a pattern of first longitudinal and then transverse, which can be roughly divided into four stages based on the diffusion

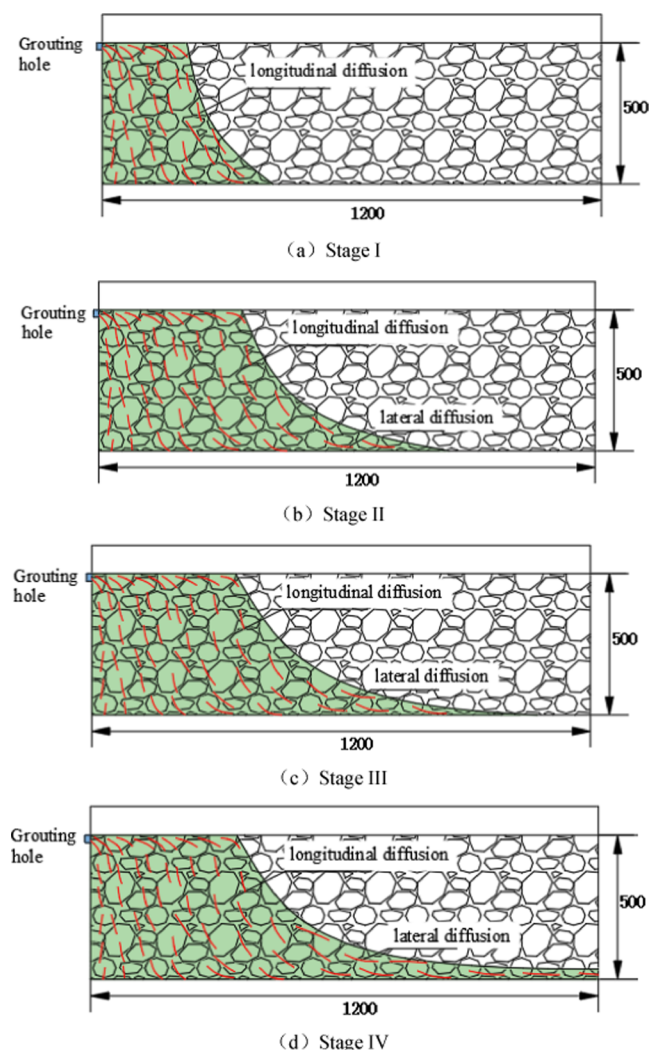


Figure 14. Diffusion process of the slurry in broken gangue (unit: mm).

characteristics of the slurry. Stage I: In the early stage of filling, the slurry forms an elliptical coverage area on the broken gangue in front of the grouting hole. As the grouting amount continues to increase, the slurry expands and infiltrates toward the bottom of the coverage area, forming a longitudinal diffusion channel near the grouting hole. Stage II: When the slurry expands and infiltrates to the bottom of the test box, it begins to flow and diffuse laterally with a certain slope. In the later stage, the slurry fills the void channel near the grouting hole from bottom to top, and the elliptical coverage area on the upper part of the test box gradually expands. Stage III: As the grouting amount continues to increase, the upper elliptical coverage area of the test box tends to stabilize, and the bottom slurry continues to diffuse laterally to the boundary of the box. Stage IV: The bottom slurry contacts the boundary of the box, and the slurry height continues to rise, but the slurry level slope remains relatively stable. When the bottom of the box leaks the slurry, grouting ends.

The liquid surface slope formed by the diffusion of the slurry during filling has a certain rule, and the closer it is to the grouting hole, the greater is the liquid surface slope. This is because the slurry near the grouting hole mainly diffuses longitudinally and the filling effect of the voids is good. The slurry accumulates, and the slope is relatively large. With the

increase in the distance from the grouting hole, the slope of the liquid surface decreases first and then tends to be stable. The void channels of slurry diffusion are randomly distributed and have different shapes, which hinders the slurry flow and diffusion. Slurry particles accumulate and settle at local small voids. Meanwhile, the surface of the gangue blocks is dry, and the slurry absorbs part of the water during diffusion, resulting in the increase of the slurry concentration and the weakening of the lateral diffusion ability.

There are stage differences in the flow and diffusion of the slurry in the voids of the crushed gangue. When the grouting hole is above the slurry level, the slurry flows around in the form of waves driven by the grouting pressure. When the grouting hole is located below the slurry level, the slurry spurts outward at the grouting hole, and the spurting slurry continuously flows and diffuses toward the surroundings. While the slurry gushes or flows outward, the slurry in the coverage area spreads downward under the action of gravity. After grouting filling, the slurry is mainly distributed in the void formed by the accumulation of rock blocks; the flow and diffusion of the slurry in the void are selective; and the flow and diffusion of the slurry are deep along the advantageous path. With the increase of the grouting amount, the slurry is filled with the void in a branched shape, successively.

5. CONCLUSIONS

- (1) The slump and bleeding rate of the filling slurry decrease continuously with the increase of the coal gangue content, while the slump and bleeding rate of the slurry decrease continuously with the increase of the fly ash content. The slump and bleeding rate of the filling slurry are inversely proportional to the gasification slag content.
- (2) The pressure change divides the grouting filling process into three stages: the initial stable stage, the step growth stage, and the pressure stability stage. The low-resistance zone refers to the zone containing a large amount of slurry, while the high-resistance zone refers to the zone containing a small amount of slurry or no slurry. That is, the low-resistance zone has a good slurry diffusion movement effect, while the high-resistance zone has a poor slurry diffusion movement effect.
- (3) During filling, the slope of the liquid surface formed by slurry diffusion presents a certain rule, and the closer the distance from the grouting hole to the liquid surface, the greater the slope. The slurry mainly spreads longitudinally near the grouting hole, the void filling effect is good, the slurry accumulation occurs, and the slope is large. At the same time, the surface of the gangue block is dry, and the slurry absorbs part of the water when it diffuses, which leads to the increase of its concentration and the weakening of its lateral diffusion ability. Secondary or multiple grouting can effectively fill the broken gangue void and further improve the filling effect of the mine.

AUTHOR INFORMATION

Corresponding Author

Wei Zhen – Institute of Energy, Hefei Comprehensive National Science Center, Hefei 230031, China; orcid.org/0000-0003-1972-7456; Email: 1961345710@qq.com

Authors

He Xiang – School of Mining Engineering, Anhui University of Science and Technology, Huainan, Anhui 232001, China; Institute of Energy, Hefei Comprehensive National Science Center, Hefei 230031, China

Yang Ke – School of Mining Engineering, Anhui University of Science and Technology, Huainan, Anhui 232001, China; Institute of Energy, Hefei Comprehensive National Science Center, Hefei 230031, China

Yu Xiang – School of Mining Engineering, Anhui University of Science and Technology, Huainan, Anhui 232001, China; Institute of Energy, Hefei Comprehensive National Science Center, Hefei 230031, China

He Shuxin – School of Mining Engineering, Anhui University of Science and Technology, Huainan, Anhui 232001, China; Institute of Energy, Hefei Comprehensive National Science Center, Hefei 230031, China

Shen Yihao – School of Mining Engineering, Anhui University of Science and Technology, Huainan, Anhui 232001, China

Liu Bin – School of Mining Engineering, Anhui University of Science and Technology, Huainan, Anhui 232001, China; Institute of Energy, Hefei Comprehensive National Science Center, Hefei 230031, China

Complete contact information is available at:

<https://pubs.acs.org/10.1021/acsomega.3c04519>

Notes

The authors declare no competing financial interest.

ACKNOWLEDGMENTS

This research was supported by the Natural Science Research Project of the Anhui Educational Committee (No. 2022AH050839); the Scientific Research Foundation for High-Level Talents of Anhui University of Science and Technology (2021yjrc11); the Institute of Energy, Hefei Comprehensive National Science Center (Nos. 21KZS217 and 21KZZ506); and the State Key Program of the National Natural Science Foundation of China (No. 52130402).

REFERENCES

- (1) Yang, K.; Wei, Z.; Zhao, X.; et al. Theory and technology of green filling of solid waste in underground mine at coal power base of Yellow River Basin. *J. China Coal Soc.* **2021**, *46*, 925–935.
- (2) Han, P.; Zhang, C.; Ren, Z.; et al. The influence of advance speed on overburden movement characteristics in longwall coal mining: insight from theoretical analysis and physical simulation. *J. Geophys. Eng.* **2021**, *18* (1), 163–176.
- (3) Feng, L. I.; Linfeng, G. U.; Luzheng, Z. H. Research on coal safety range and green low-carbon technology path under the dual-carbon background. *J. China Coal Soc.* **2022**, *47* (1), 1–15.
- (4) Yang, K.; Zhao, X.; Zhen, W.; et al. Development overview of paste backfill technology in China's coal mines: a review. *Environ. Sci. Pollut. Res.* **2021**, *28*, 67957–67969.
- (5) Wang, J.; Liu, T. Feasibility study on the technology of filling the vacant space of the caving rock with cement materials. *Coal Min.* **2001**, *1*, 44–45.
- (6) Jiang, N.; Zhao, J.; Sun, X.; et al. Use of fly-ash slurry in backfill grouting in coal mines. *Heliyon* **2017**, *3* (11), No. e00470, DOI: 10.1016/j.heliyon.2017.e00470.
- (7) Yang, Y. *Study of Mechanism of Controlling the Overlying Rock by Injecting Ash Thick Liquid into the Mining Collapse Zone*, Liaoning Technical University: 2007.
- (8) Li, L.; Huang, Q.; Wu, J.; et al. Underground treatment of coal gangue and fluidization filling technology in caving area. *J. Xi'an Univ. Sci. Technol.* **2022**, *42* (5), 865–873.
- (9) Li, X.; Xu, J.; Zhu, W.; et al. Simulation of backfill compaction character by particle flow code. *J. China Coal Soc.* **2008**, *163* (4), 373–377.
- (10) Zhang, J.; Zhang, Q.; Spearing, A. J. S. Sam.; et al. Green coal mining technique integrating mining-dressing-gas draining-backfilling-mining. *Int. J. Min. Sci. Technol.* **2017**, *27* (1), 17–27.
- (11) Zhao, W.; Shao, H. Instant detection method of grouting effect in deep mine goaf. *J. China Coal Soc.* **2021**, *46* (S2), 621–628.
- (12) Wang, Q.; Zhu, Y.; Li, W.; et al. Study on the mechanism of column permeation grouting of Bingham fluid considering the spatial attenuation of viscosity. *Chin. J. Rock Mech. Eng.* **2022**, *41* (8), 1647–1658.
- (13) Qian, Z.; Jiang, Z.; Cao, L.; et al. Experiment study of penetration grouting model for weakly cemented porous media. *Rock Soil Mech.* **2013**, *34* (1), 139–142.
- (14) Qing-song, Z.; Lian-zhen, Z.; Ren-tai, L.; et al. Split grouting theory based on slurry-soil coupling effects. *Chin. J. Geotech. Eng.* **2016**, *38* (2), 323–330.
- (15) Liu, F.; Ma, H.; Yin, X. Application of fracture grouting in airport road extension. *Subgrade Eng.* **2015**, *181* (4), 163–167.
- (16) Shuming, Z.; Jianjun, C. H. Hydrofracture grouting in soft flowing mucky ground for a metro tunnel. *Chin. J. Geotech. Eng.* **2002**, *24* (2), 222–224.
- (17) Hu, S.; Liu, Q.; Li, S.; et al. Advance and review on grouting critical problems in fractured rock mass. *Coal Sci. Technol.* **2022**, *50* (1), 112–126.
- (18) Yang, X. *Study on Grout Diffusion Theory and Experiments under Static or Dynamic Loading*; Central South University, 2005.
- (19) Feng, Z. *Material Development and Research of Osmosis and Diffusion on Chemical Grouting for Extraordinary Cracked Coal and Rockmass*; China Coal Research Institute, 2007.
- (20) Miwen, G.; Wanghua, S. Design of model test system for grouting under high pressure conditions. *J. Eng. Geol.* **2010**, *18* (5), 720–724.
- (21) Zhang, D. *Investigation on Coupling Mechanism of Multi-fields for Grouting Diffusion in Fractured Rock Mass with Flowing Water*; China University of Mining and Technology, 2018.
- (22) Li, S.; Bu, L.; Shi, S.; et al. Prediction for water inrush disaster source and CFD-based design of evacuation routes in karst tunnel. *Int. J. Geomech.* **2022**, *22* (5), 1–12.
- (23) Wang, X.; Liu, R.; Yang, W.; et al. Study on grouting mechanism of horizontal fractures considering the bleeding of cement slurry. *Chin. J. Rock Mech. Eng.* **2019**, *38* (5), 1005–1017.
- (24) Sha, F.; Li, S.; Liu, R.; et al. Experimental study on performance of cement-based grouts admixed with fly ash, bentonite, superplasticizer and water glass. *Constr. Build. Mater.* **2018**, *161*, 282–291.
- (25) Zhang, G.; Zhan, K.; Sui, W. Experimental investigation of the impact of flow velocity on grout propagation during chemical grouting into a fracture with flowing water. *J. China Coal Soc.* **2011**, *36* (3), 403–406.
- (26) Ao, X.; Wang, X.; Zhu, X.; et al. Grouting Simulation and Stability Analysis of Coal Mine Goaf Considering Hydromechanical Coupling. *J. Comput. Civil Eng.* **2016**, *31* (3), 1–17, DOI: 10.1061/(ASCE)CP.1943-5487.0000640.
- (27) Zou, Y. *The Mechanism and Application of the Goaf Grouting with High Addition Fly Ash in Coal Mine*; China Coal Research Institute, 2016.
- (28) Zhu, L.; Pan, H.; Gu, W.; et al. Experimental study on flow and diffusion law of gangue filling slurry in caving zone. *J. China Coal Soc.* **2021**, *46* (S2), 629–638.
- (29) Qiu, H.; Liu, L.; Sun, W.; et al. Experimental study on strength distribution of backfill in goaf. *J. Cent. South Univ.* **2018**, *49* (10), 2584–2592.
- (30) GB 15618-2018. Soil Environmental Quality Standard for Soil Pollution Risk Control of Agricultural Land (Trial).
- (31) Wu, F.; Yang, F.; Xiao, B.; et al. Characterization of rheological property and its application of high concentration and mixed aggregate filling slurry based on spread. *J. Cent. South Univ.* **2022**, *53* (8), 3104–3112.

- (32) Zhu-en, R.; Ai-xiang, W.; Yi-ming, W.; et al. Multiple response optimization of key performance indicators of cemented paste backfill of total solid waste. *Chin. J. Eng.* **2022**, *44* (4), 496–503.
- (33) Zhang, C.; Zhao, Y. X.; Bai, Q. S. 3D DEM method for compaction and breakage characteristics simulation of broken rock mass in goaf. *Acta Geotech.* **2022**, *17* (7), 2765–2781.
- (34) Zhang, C.; Zhang, L. Permeability characteristics of broken coal and rock under cyclic loading and unloading. *Nat. Resour. Res.* **2019**, *28* (3), 1055–1069.
- (35) Kong, X.; Wang, E.; He, X.; et al. Mechanical characteristics and dynamic damage evolution mechanism of coal samples in compressive loading experiments. *Eng. Fract. Mech.* **2018**, *210* (S1), 160–169.
- (36) Liu, Y.; Cheng, J.; Jiao, J.; et al. Feasibility study on mutil-seam upward mining of multi-layer soft-hard alternate complex roof. *Environ. Earth Sci.* **2022**, *81* (17), 1–20.
- (37) Hu, Q.; Hu, M.; Li, Q.; et al. Analysis of resistivity response of stratified briquette during uniaxial compression. *J. China Coal Soc.* **2021**, *46* (01), 211–219.
- (38) Guo, Y.; Zhao, Y.; Feng, G.; et al. Study on damage size effect of cemented gangue backfill body under uniaxial compression. *Chin. J. Rock Mech. Eng.* **2021**, *40* (12), 2434–2444.
- (39) Cai, W.; Chang, Z.; Zhang, D.; et al. Roof filling control technology and application to mine roadway damage in small pit goaf. *Int. J. Min. Sci. Technol.* **2019**, *29* (3), 477–482.
- (40) Yun, L.; Lijun, H. A.; Sun, C.; Yemao, D. O.; et al. Experiment study on secondary grouting reinforcement of broken surrounding rock in large loose circle. *Coal Sci. Technol.* **2012**, *40* (12), 19–23.
- (41) Li, C.; Wu, Z.; Zhang, W.; et al. A case study on asymmetric deformation mechanism of the reserved roadway under mining influences and its control techniques. *Geomech. Geoeng.* **2020**, *22* (5), 449–460.